Comparison of Sensor and Sensor-less Vector Control Techniques for Induction Motor in EOT Crane Low Speed Applications

K.Seshubabu and C.L. Jose

Satish Dhawan Space Centre, SHAR, Sriharikota

Abstract: This paper presents a comparison between Sensor or Indirect Field Oriented Control (IFOC) and Sensor-less Field Oriented Control (SFOC) in low frequency region for Induction Motor (IM). These two strategies can be considered among the family of Vector Control (VC) methods and provide a solution for high-performance drives. Most of the Electrically-operated Overhead Travelling (EOT) Crane IMs are controlled with vector control techniques. IM performance will deteriorate as frequency falls below 5 Hz due to its stator resistance drop. There are some critical requirements which needs rocket segments and satellite needs to be positioned in very precise position. For this EOT crane has to run in creep speed which needs drive has to run below 5 Hz. In this paper, the analysis is carried out on IFOC and SFOC methods and implemented to IM drives. In IFOC, flux magnitude and angle is achieved by imposing a slip frequency derived from the rotor dynamic equations with monitored rotor speed using external sensor such as encoder. Whereas SFOC does not require any sensor for estimation of flux magnitude and position, with monitored stator voltages and stator currents, flux magnitude and position can be achieved. Advantages and disadvantages of two control methods are emphasized in low frequency region (0-5 Hz). The theoretical results are found to be consistent with experimental results performed on 100 HP, three phase IM. It is concluded that IFOC method is better than SFOC method in low frequency region.

Keywords: IFOC, SFOC, Vector Control, Induction Motor, low frequency region.

I. Introduction

Variable-speed alternating current (AC) drives have been used in the past to perform relatively undemanding roles in applications which preclude the use of direct current (DC) motors, either because of the working environment or commutator limits. Vector control or Field Orientation Control (FOC) techniques [1] incorporating fast microprocessors and DSPs have made possible the application of induction motor (IM) for high-performance applications where traditionally only DC drives were applied. In FOC, the current space vector is controlled both in magnitude and position to achieve decoupled control of the torque producing and the flux producing components of the stator current space phasor. To achieve decoupled control, either the stator flux, airgap flux or the rotor flux should be known both in magnitude and position. Two possible methods for achieving field orientation were identified. Blaschke [2] used Hall sensors mounted in the air gap to measure the machine flux, and therefore obtain the flux magnitude and flux angle for field orientation. Field orientation achieved by direct measurement of the flux is termed Direct Flux Orientation Control (DFOC) [3]-[5]. On the other hand Hasse [6] achieved flux orientation by imposing a slip frequency derived from the rotor dynamic equations with monitored rotor angle using encoder so as to ensure field orientation. This alternative, consisting of forcing field orientation in the machine, is known as Indirect Field Orientation Control (IFOC) [7]-[9]. IFOC has been generally preferred to DFOC implementations which use Hall probes; the reason being that DFOC requires a specially modified machine and moreover the fragility of the Hall sensors detracts the inherent robustness of an induction machine. However the typical IFOC requires the use of an accurate shaft encoder for correct operation which gives additional cost. Therefore there has been great interest in the research community in developing a high performance induction motor drive that does not require a speed or position transducer for its operation. Sensor-less Field Oriented

Received: August 7th, 2015. Accepted: March 23rd, 2017

DOI: 10.15676/ijeei.2017.9.1.5

Control (SFOC) of induction motor does not require any sensor for estimation of flux magnitude and position [10]-[15]. By using the speed estimation techniques, the information of speed can be estimated from measured stator voltages and currents and this information is feedback to control of the induction motor drive. Some kind of speed estimation is required for high performance motor drives, in order to perform speed control. Alternatively, speed information can be obtained by using a machine model fed by stator quantities. These include the use of simple open loop speed calculators, Model Reference Adaptive Systems (MRAS) and Extended Kalman Filters [16]-[18]. All of these methods are parameter dependent, therefore parameter errors can degrade speed holding characteristics. In certain industrial applications such as cranes, motion control and traction applications, requirement of precise mechanical position is much essential which necessitates IM to run in low frequency region with constant torque. In low frequency region (0-5 Hz), stator voltage drop is comparable with applied voltage which reduces the airgap-flux in constant torque.

Several papers have been published on IFOC and SFOC techniques [19]-[20], but only few of them only compared in general perspective. The aim of this paper is to give a comparison between IFOC and SFOC in low frequency region emphasizing advantages and disadvantages. Theoretical analysis and experimental tests have been carried out on 100 HP motor which is used for hoist operation in 60t Electrically-operated Overhead Travelling (EOT) crane. This EOT crane hoist motor is controlled with Variable Voltage Variable Frequency Drive (VVVF). Operation of the EOT crane with VVVF drives is much critical and is used for handling rocket segments during vehicle assembly integration activities. The employed technique should not cause any vibration or motor heating during precise operation. The comparison is useful to indicate to the users which one of the two schemes can be efficiently employed in the various applications based on torque control requirement.

2. IFOC and SFOC Techniques

A. IFOC Technique

In this method, the stator currents of the induction machine can be decoupled into flux and torque producing components with rotating vectors in a complex coordinate system. In this case, the stator current components are transformed into a new rotating reference frame, which rotates together with a selected flux-linkage space vector. In this context rotor flux linage vector was selected which is termed as Rotor Flux FOC. The implementation of the rotor flux FOC requires information on the modulus and space angle (position) of the rotor flux-linkage space phasor which can be obtained by utilizing the monitored stator currents and rotor speed from encoder. In ac machine electromagnetic torque can be expressed as

$$t_e = k\,\bar{\Psi}_s \mathrm{X} \bar{\iota}_r{}' \text{ or } t_e = k\,\bar{\Psi}_s{}' \mathrm{X} \bar{\iota}_r \quad (1)$$

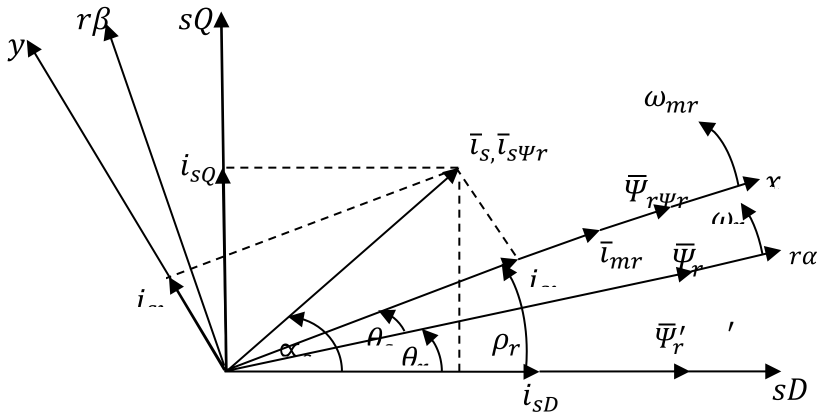

Figure 1. Stator current and rotor flux-linkage space phasors in the general reference frame which is fixed to the rotor flux-linkage space phasor

However, if instead of a reference frame fixed to the stator and rotor, a general reference frame with direct and quadrature axes x, y rotating at a general instantaneous speed ($\omega_{mr} = \frac{d\rho_r}{dt}$) which is fixed to the rotor flux linkage space phasor as shown in Figure1. Torque can be expressed as vector product of the rotor flux linkage and the stator current space phasors. The rotor flux-linkage space phasor in the general reference frame can be expressed as

$$\bar{\Psi}_{r\Psi r} = L_r \bar{\imath}_{r\Psi r} + L_m \bar{\imath}_{s\Psi r} = \bar{\Psi}_r e^{-j(\rho_r-\theta_r)} = \bar{\Psi}_r e^{j\theta_r} e^{-j\rho_r} = \bar{\Psi}_r{}' e^{-j\rho_r} = |\bar{\Psi}_r| e^{j\rho_r} e^{-j\rho_r} = |\bar{\Psi}_r| = \Psi_{rx} \quad (2)$$

The stator current in the general reference frame can be expressed as

$$\bar{\imath}_{s\Psi r} = \bar{\imath}_s e^{-j\rho_r} = i_{sx} + j i_{sy} \quad (3)$$

Electromagnetic torque can be expressed in general reference frame as

$$t_e = k\, \bar{\Psi}_{r\Psi r} \mathrm{X} \bar{\imath}_{s\Psi r} = \frac{3}{2} P \frac{L_m}{L_r} \Psi_{rx} i_{sy} \; (\because\; \bar{\Psi}_{r\Psi r} = L_r \bar{\imath}_{r\Psi r} + L_m \bar{\imath}_{s\Psi r} = |\bar{\Psi}_r| = \Psi_{rx}) \quad (4)$$

The relationship between the stator current components in the stationary reference frame (i_{sD}, i_{sQ}) and the stator current components in the general reference frame (i_{sx}, i_{sy}) can be obtained as

$$\begin{bmatrix} i_{sx} \\ i_{sy} \end{bmatrix} = \begin{bmatrix} \cos\rho_r & \sin\rho_r \\ -sin\rho_r & cos\rho_r \end{bmatrix} \begin{bmatrix} i_{sD} \\ i_{sQ} \end{bmatrix} \quad (5)$$

Rotor magnetizing current in the general reference frame is defined in terms of stator and rotor-current space phasors given by

$$\bar{\imath}_{mr} = i_{mrx} + j i_{mry} = \frac{\bar{\Psi}_{r\Psi r}}{L_m} = \frac{\Psi_{rx}}{L_m} = i_{mrx} = |\bar{\imath}_{mr}| = \frac{L_r \bar{\imath}_{r\Psi r} + L_m \bar{\imath}_{s\Psi r}}{L_m} = \frac{L_r}{L_m} \bar{\imath}_{r\Psi r} + \bar{\imath}_{s\Psi r}$$

$$= \bar{\imath}_{s\Psi r} + (1+\sigma_r)\, \bar{\imath}_{r\Psi r} \text{Where } \sigma_r = \frac{L_{rl}}{L_m} \; and \; L_r = L_{rl} + L_m \quad (6)$$

Thereby torque eqn. can be represented as

$$t_e = \frac{3}{2} P \frac{L_m^2}{L_r} |\bar{\imath}_{mr}| i_{sy} = \frac{3}{2} P \frac{L_m}{1+\sigma_r} |\bar{\imath}_{mr}| i_{sy} \quad (7)$$

Eqn. 7, shows that electromagnetic torque can be controlled by independently controlling the flux-producing current component $|\bar{\imath}_{mr}|$ and torque-producing stator current component i_{sy}. Under linear magnetic conditions L_m, L_r and the term $\frac{3}{2} P \frac{L_m}{1+\sigma_r}$ are constant, and the expression for the torque is similar to that of the separately excited dc machine.

The rotor voltage equation of the induction machine in general reference frame can be expressed as

$$R_r \bar{\imath}_{r\Psi r} + \frac{d\,\bar{\Psi}_{r\Psi r}}{dt} + j(\omega_{mr} - \omega_r)\, \bar{\Psi}_{r\Psi r} = 0 \quad (8)$$

$$R_r \bar{\imath}_{r\Psi r} + L_m \frac{d|\bar{\imath}_{mr}|}{dt} + j(\omega_{mr} - \omega_r) L_m |\bar{\imath}_{mr}| = 0 \; (\because\; \bar{\Psi}_{r\Psi r} = \bar{\Psi}_r e^{-j(\rho_r-\theta_r)} = L_m |\bar{\imath}_{mr}|) \quad (9)$$

And from the above

$$T_r \frac{d|\bar{\imath}_{mr}|}{dt} + |\bar{\imath}_{mr}| = \bar{\imath}_{s\Psi r} - j(\omega_{mr} - \omega_r) T_r |\bar{\imath}_{mr}| \quad (10)$$

$$T_r \frac{d|\bar{\imath}_{mr}|}{dt} + |\bar{\imath}_{mr}| = i_{sx} \tag{11}$$

$$\omega_{mr} = \omega_r + \frac{i_{sy}}{T_r|\bar{\imath}_{mr}|} \tag{12}$$

In eqn. (12) the term $\frac{i_{sy}}{T_r|\bar{\imath}_{mr}|}$ represents the angular rotor frequency (angular slip frequency of the rotor flux) $\omega_{sl,}$and it follows that the angular speed of the rotor flux is equal to the sum of the angular rotor speed and the angular slip frequency of the rotor flux. If $|\bar{\imath}_{mr}|$ is constant, it follows from eqn (11), that $|\bar{\imath}_{mr}| = i_{sx}$, the modulus of the rotor flux-linkage space phasor can be kept at a desired level by controlling the direct-axis stator current i_{sx}, the electromagnetic torque is determined by the quadrature-axis stator current i_{sy}.

In indirect rotor filed-oriented control method, the space angle of the rotor flux-linkage space phasor (ρ_r) is obtained as the sum of the monitored rotor angle (θ_r) and the computed reference value of the slip angle(θ_{sl}), where the slip angle gives the position of the rotor flux-linkage space phasor relative to the rotor. These angles are shown in Figure1. The required equations follow from eqn. (2), according to which the speed of the rotor magnetizing current space phasor is

$$\omega_{mr} = \omega_r + \omega_{slref} \tag{13}$$

Where ω_r is the rotor speed,

$$\omega_r = \frac{d\theta_r}{dt} \tag{14}$$

and ω_{slref} is the reference value of the slip frequency,

$$\omega_{slref} = \frac{i_{sy}}{T_r|\bar{\imath}_{mr}|} \tag{15}$$

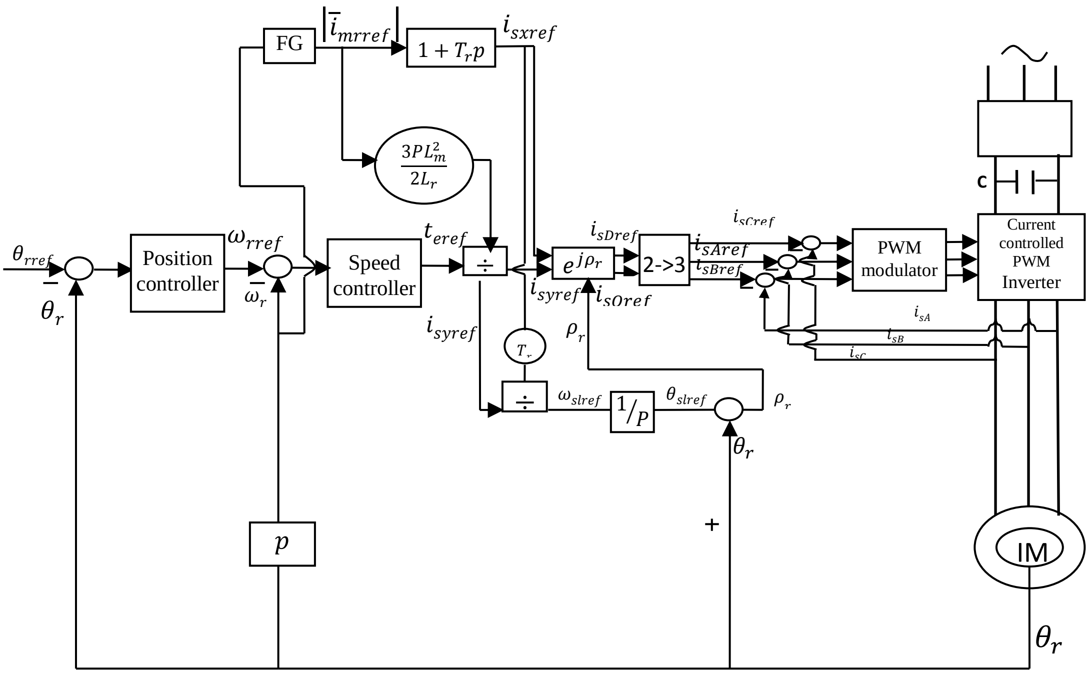

Figure 2. Schematic of the Indirect rotor-flux-oriented control of current-controlled PWM inverter-fed induction motor

Furthermore

$$\omega_{mr} = \frac{d\rho_r}{dt} \tag{16}$$

Thus it follows from eqns. (13)-(16) that

$$\rho_r = \int \omega_{mr} dt = \int \left(\omega_r + \omega_{slref}\right) dt = \theta_r + \theta_{slref} \tag{17}$$

The slip angle θ_{slref} gives the position of the rotor magnetizing-current space phasor with respect to the direct-axis of the reference frame fixed to the rotor.

$$\rho_r = \theta_r + \int \omega_{slref} dt = \theta_r + \int \frac{i_{sy}}{T_r |\bar{\imath}_{mr}|} dt \tag{18}$$

Which serves as the basis for obtaining the angle ρ_r in the implementation of the rotor-flux-oriented control of induction machine. According to eqn. (18) the division of the direct and quadrature axis stator currents $(i_{sxref,} i_{syref})$ is controlled by the slip frequency ω_{sl} and the two reference currents are used to determine the required slip frequency. When the rotor angle and reference value of the slip frequency angle are added, the position of the rotor magnetizing-current space phasor is obtained.

The schematic of the drive is shown in Figure 2. An incremental rotor position sensor is used to obtain the rotor angle (θ_r) and the rotor speed (ω_r). The actual value of the rotor angle (θ_r) is compared with its reference value (θ_{ref}) and the resulting error serves as the input to the position controller, which is a PI controller. The output of the position controller is the reference value of the rotor speed (ω_{rref}). This is compared with the monitored value of the rotor speed and the error is supplied as the input to the speed controller. Its output is the reference value of the electromagnetic torque (t_{eref}) and this is divided by the constant $\frac{3}{2} P \frac{L_m^2}{L_r}$ to yield the reference value of the stator current expressed in the rotor-flux-oriented reference frame $\left(i_{syref}\right)$. The monitored rotor speed serves as the input to the function generator FG gives a reference value of the rotor magnetizing current $\left(|\bar{\imath}_{mrref}|\right)$.

B. SFOC Technique-

Similar to IFOC technique, in this method also the stator currents of the induction machine can be decoupled into flux and torque producing components with rotating vectors in a complex coordinate system. Stator current components are transformed into a new rotating reference frame, which rotates together with stator-flux-linkage space vector, which is termed as Stator flux Field Oriented Control. The implementation of the stator flux FOC requires information on the modulus and space angle (position) of the stator flux-linkage space phasor which can be obtained by utilizing the monitored stator currents and voltages. Since in this there is no sensor used for monitoring rotor speed and rotor speed can be calculated by different estimation techniques. This technique also called as Sensor-less Field-Oriented Control (SFOC). In the stationary reference frame the space phasor of the stator flux linkages can be expressed as

$$\bar{\Psi}_s = \Psi_{sD} + j\Psi_{sQ} = \int (\bar{u}_s - R_s \bar{\imath}_s)\, dt \tag{19}$$

Where

$$\Psi_{sD} = \int (u_{sD} - R_s i_{sD}) \mathrm{dt}$$
$$\Psi_{sQ} = \int (u_{sQ} - R_s i_{sQ}) \mathrm{dt}$$

A general reference frame with direct and quadrature axes x, y rotating at a general instantaneous speed $(\omega_{ms} = \frac{d\rho_s}{dt})$ which is fixed to the stator flux orientation as shown in

Figure 3 and ρ_s is a spatial angle with respect to the real axis of the stationary reference frame (sD).

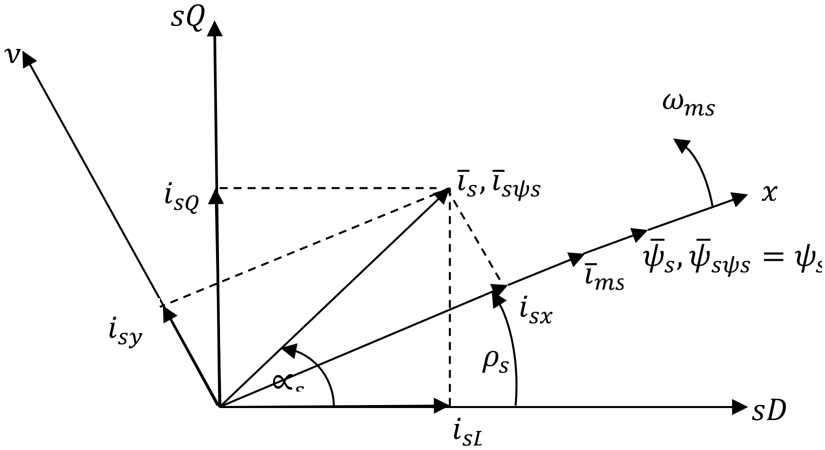

Figure 3. Relation between the stationary reference frame and the general reference frame fixed to the stator flux-linkage space phasor

Figure 3 shows the relationship between the general and the stationary reference frame. The space phasors of the stator current and stator current and the stator flux linkages are

$$\bar{\iota}_{s\Psi s} = \bar{\iota}_s e^{-j\rho_s} = (i_{sD} + ji_{sQ})e^{-j\rho_s} = i_{sx} + ji_{sy} \tag{20}$$

$$\bar{\Psi}_{s\Psi s} = \bar{\Psi}_s e^{-j\rho_s} = (\Psi_{sD} + j\Psi_{sQ})e^{-j\rho_s} = \Psi_{sx} + j\Psi_{sy} = |\bar{\Psi}_s|e^{j\rho_s}e^{-j\rho_s} = |\bar{\Psi}_s| = \Psi_{sx} \tag{21}$$

and

$$\begin{bmatrix} i_{sx} \\ i_{sy} \end{bmatrix} = \begin{bmatrix} \cos\rho_s & \sin\rho_s \\ -sin\rho_s & cos\rho_s \end{bmatrix} \begin{bmatrix} i_{sD} \\ i_{sQ} \end{bmatrix} \tag{22}$$

Which gives the relationship of i_{sD}, i_{sQ} and the transformed currents i_{sx}, i_{sy}.
The space phasor of the stator flux linkages in the general reference frame is expressed in terms of the stator and rotor currents can be expressed as

$$\bar{\Psi}_{s\Psi s} = L_s\bar{\iota}_{s\Psi s} + L_m\bar{\iota}_{r\Psi s} \tag{23}$$

The stator magnetizing current $\bar{\iota}_{ms}$ in the general reference frame can be expressed as

$$\bar{\iota}_{ms} = i_{msx} + ji_{msy} = \frac{\bar{\Psi}_{s\Psi s}}{L_m} = \frac{\Psi_{sx}}{L_m} = i_{msx} = |\bar{\iota}_{ms}| = \frac{L_s}{L_m}\bar{\iota}_{s\Psi s} + \bar{\iota}_{r\Psi s} = (1+\sigma_s)\bar{\iota}_{s\Psi s} + \bar{\iota}_{r\Psi s} \tag{24}$$

The electromagnetic torque can be expressed as

$$t_e = \frac{3}{2}P\bar{\Psi}_{s\Psi s}\text{X}\,\bar{\iota}_{s\Psi s} = \frac{3}{2}P|\bar{\Psi}_s|i_{sy} = \frac{3}{2}PL_m|\bar{\iota}_{ms}|i_{sy} \tag{25}$$

The stator-voltage equation expressed in the stator-flux-oriented reference, which rotates at the speed of the stator flux-linkage space vector ($\omega_{ms} = \frac{d\rho_s}{dt}$), can be expressed as

$$\bar{u}_{s\Psi s} = R_s\bar{\iota}_{s\Psi s} + \frac{d|\bar{\Psi}_s|}{dt} + j\omega_{ms}|\bar{\Psi}_s| \tag{26}$$

By separating real and imaginary components

$$\frac{d|\bar{\Psi}_s|}{dt} = u_{sx} - R_s i_{sx} \tag{27}$$

And the speed of the stator-flux space vector is obtained as

$$\omega_{ms} = \frac{u_{sy} - R_s i_{sy}}{|\bar{\Psi}_s|} \tag{28}$$

From Eqn. (28) $|\bar{\Psi}_s|$ can be estimated from $\int (u_{sx} - R_s i_{sx})\, dt$ and the angle ρ_s can be obtained by the integration of ω_{ms}. For estimation of rotor speed, rotor voltage space vector equation in stationary reference frame can be expressed as

$$R_r i_{rd} + \frac{d\psi_{rd}}{dt} + \omega_r \psi_{rq} = 0 \tag{29}$$

Where $\psi_{rd} = L_r i_{rd} + L_m i_{sD}$ (30)

ψ_{rd}, ψ_{rq} and i_{rd}, i_{rq} are instantaneous values of direct- and quadrature-axis rotor flux linkage components and rotor current components respectively expressed in the stator reference frame. Space phasor of the rotor flux linkages expressed in the stator reference frame can be expressed as

$$\bar{\Psi}_r{}' = \psi_{rd} + j\psi_{rq} \tag{31}$$

and

$$\bar{\Psi}_r{}' = \frac{L_r}{L_m}(\bar{\Psi}_s - L_s' \bar{\iota}_s) \tag{32}$$

rotor speed can be expressed as

$$\omega_r = \left[-\frac{d\psi_{rd}}{dt} - \frac{\psi_{rd}}{T_r} + \frac{L_m}{T_r} i_{sD}\right] / \Psi_{rq} \tag{33}$$

Figure 6 shows the stator flux model in stator-flux-oriented reference frame. This model is derived from eqns. (30)-(47).

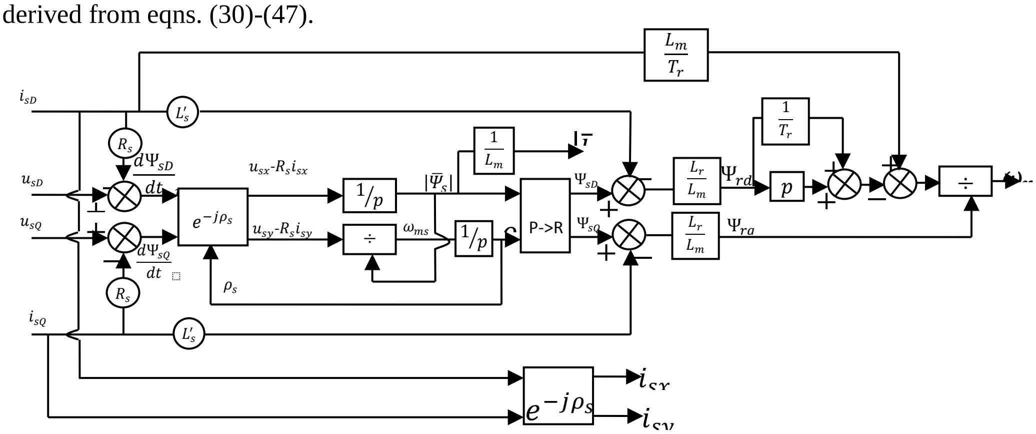

Figure 6. Stator flux model in stator-flux-oriented reference frame

The schematic of the drive using SFOC technique is shown in Figure 7. In place of encoder, stator flux model is used for rotor speed estimation. Inputs for stator flux model is monitored stator voltages and stator currents. Outputs from the model is stator magnetizing current, space angle of the stator flux linkage space vector, rotor speed and stator quadrature axis current component. The reference value of the rotor speed (ω_{rref}) is compared with the estimated value of the rotor speed (ω_r) and the error is supplied as the input to the speed controller. Its output is the reference value of the electromagnetic torque (t_{eref}) and $\frac{3}{2} P L_m |\bar{\iota}_{ms}| i_{sy}$ gives the estimated value of the rotor torque (t_e) and the error is supplied to the torque controller to yield the reference value of the stator quadrature current expressed in the stator-flux-oriented reference frame (i_{syref}). The estimated stator magnetizing current ($|\bar{\iota}_{ms}|$) and reference value of the magnetizing current ($|\bar{\imath}_{msref}|$) serves as input to the flux controller gives a reference value of the stator current along the real axis of the stator-flux-oriented reference frame (i_{sxref}).

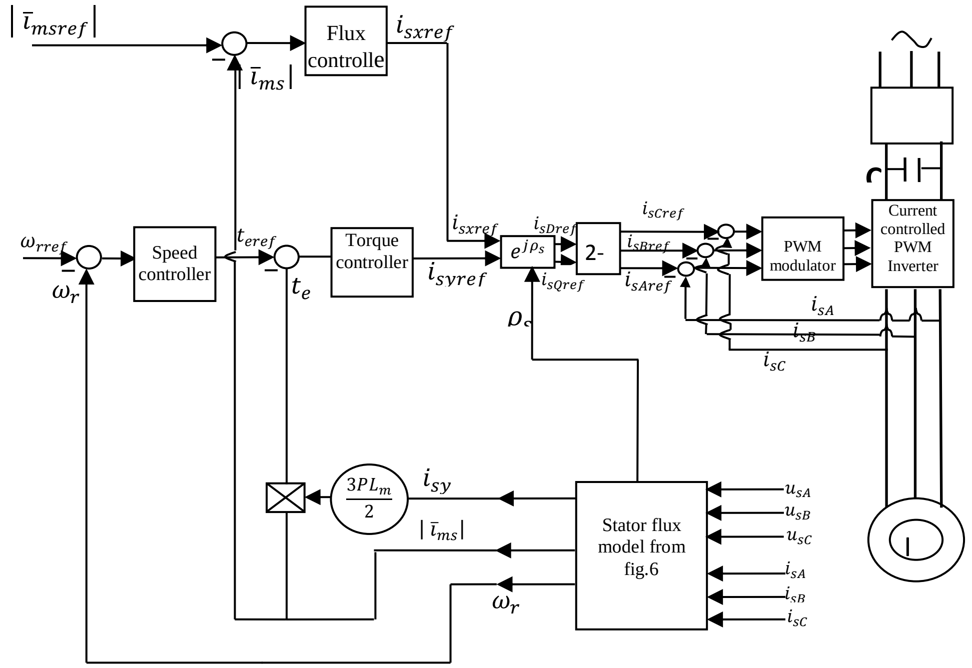

Figure7 Schematic of the Stator flux field oriented control of current-controlled PWM inverter-fed induction motor

3. Comparison between IFOC and SFOC Techniques in low frequency region

In SFOC technique, constant airgap flux will maintain if the stator voltage drop is negligible. This condition is reasonably well satisfied near rated motor frequency, but the stator ohmic voltage drop(IR) that is developed by the rated motor current remains constant as the frequency is reduced, so that at low frequencies, this IR drop is a large portion of the terminal voltage. Thus, if the stator IRdrop at rated frequency and full load is 4 percent of the phase voltage, the effect on air gap flux is relatively insignificant. However, at one tenth of rated frequency, with a constant volts/hertz supply, the IR drop at rated current is 40 percent of the applied voltage, causing a significant reduction in air gap mmf and flux. Consequently, for motoring operation, there is severe under-excitation at low speeds and intolerable loss of torque capability. This problem is resolved by implementing a terminal voltage/frequency characteristic in which the voltage is boosted above its frequency- proportional value at low frequencies in order to compensate for the stator IR drop which is shown in Figure 7. In IFOC technique, as slip frequency is constant for constant torque at different frequencies, the required voltage which is proportional to rotor angle from encoder feedback is only applied. Where as in SFOC, at low frequencies, stator resistance drop is comparable with applied voltage, there is a reduction of stator flux linkage space phasor magnitude($|\bar{\Psi}_s|$), which will reduce torque (t_e) and rotor speed (ω_r). For compensating stator IR drop, a fixed amount of voltage will be applied due to no feedback from rotor speed. This additional voltage will give full load torque and produce full load current at no load which creates magnetic saturation. However, this large boost may cause overheating if the motor operates for long periods at low speeds when the effectiveness of the internal cooling fan is significantly reduced which results higher thermal motor stressing. Since rotor speed is determined from the position of the stator flux linkage space vector, this technique mainly depends upon the accuracy of the estimated stator flux-linkage components and these depend on the precision of the monitored voltages and currents, and also on integration techniques. For accurate flux-linkage estimation, the stator resistance must be adapted to temperature changes. The integration can become problematic at low frequencies, where the stator voltages become very small and are dominated by the ohmic voltage drops.

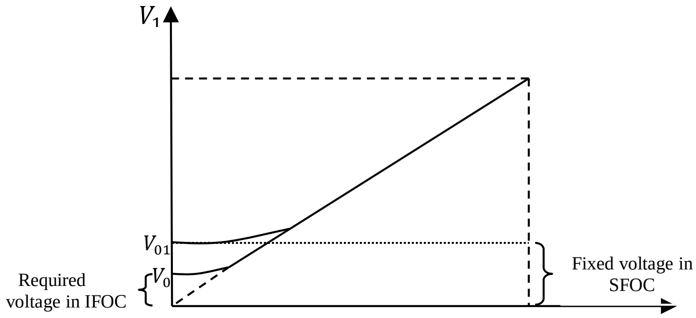

Figure 7. v/f characterstics with IFOC and SFOC

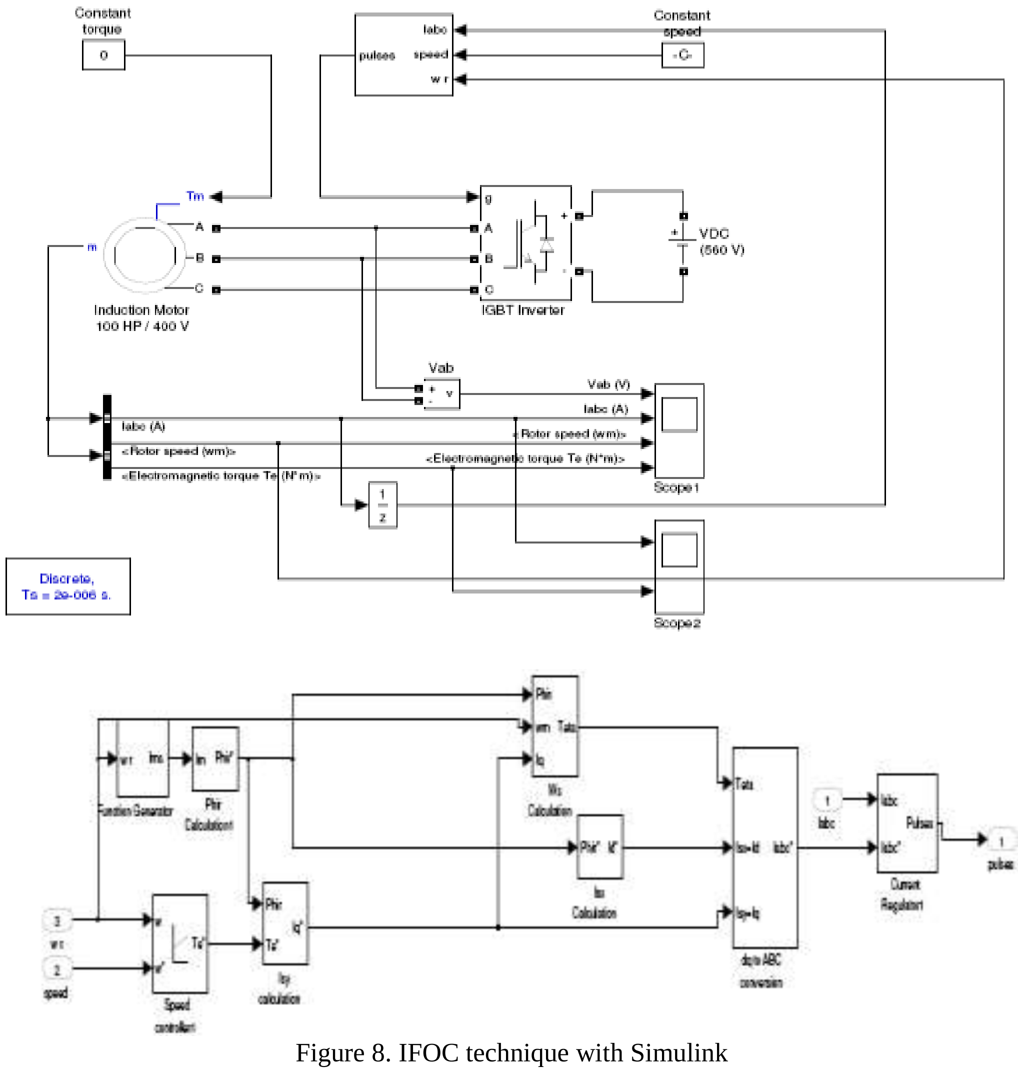

Figure 8. IFOC technique with Simulink

4. MATLAB Simulation

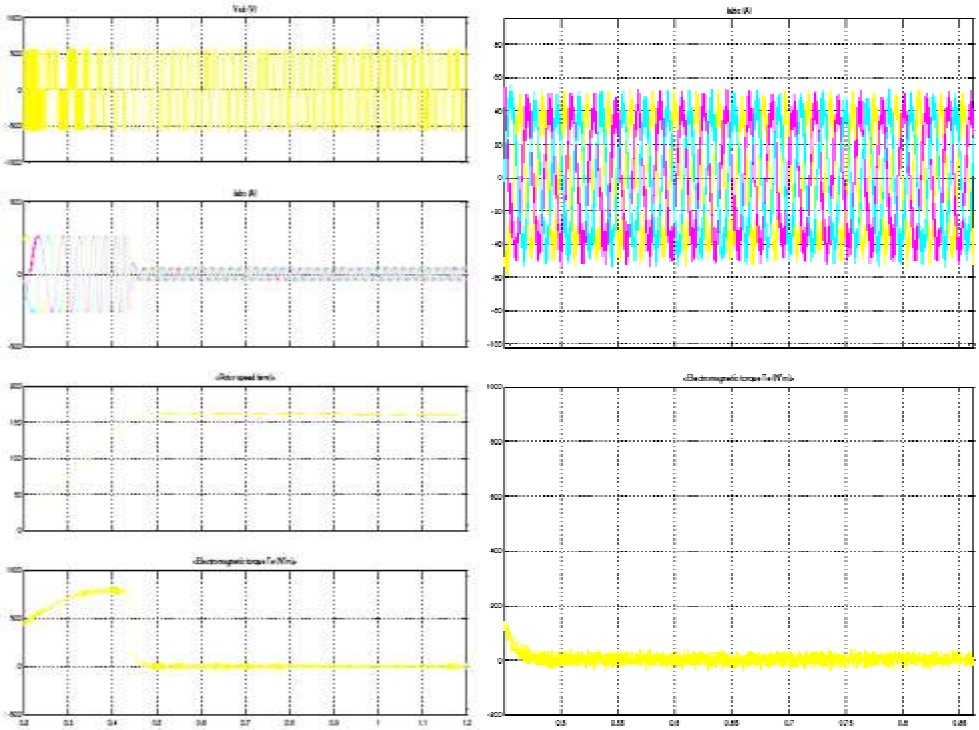

Figure 9. a) IFOC: V, I, N and T at 50 Hz b) IFOC: I and T at 50 Hz

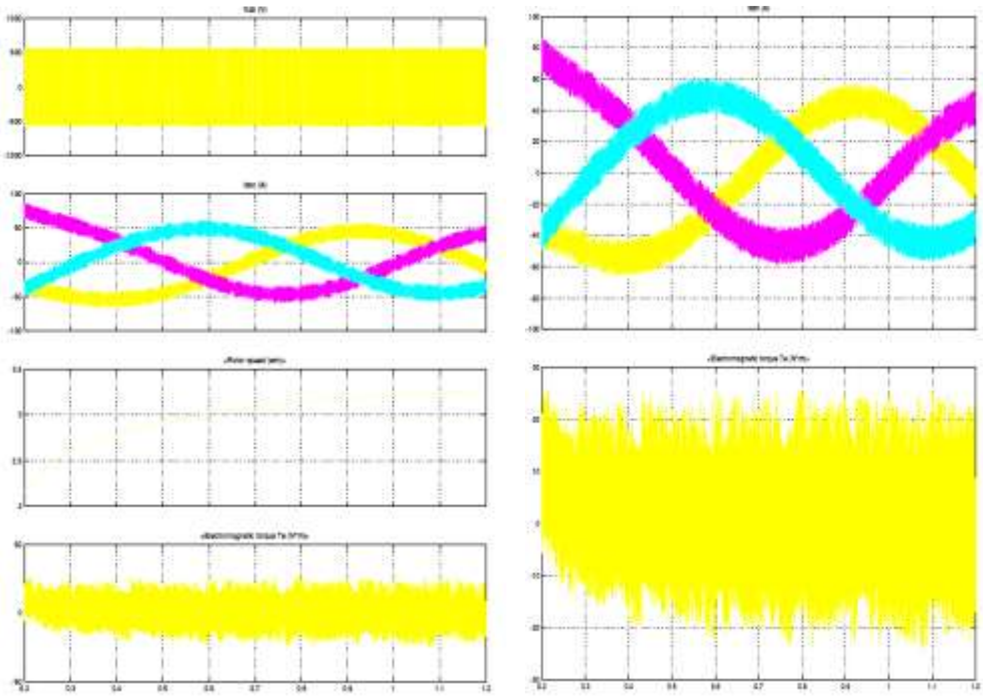

Figure10 a) IFOC: V, I, N and T at 1 Hz b)IFOC: I and T at 1 Hz

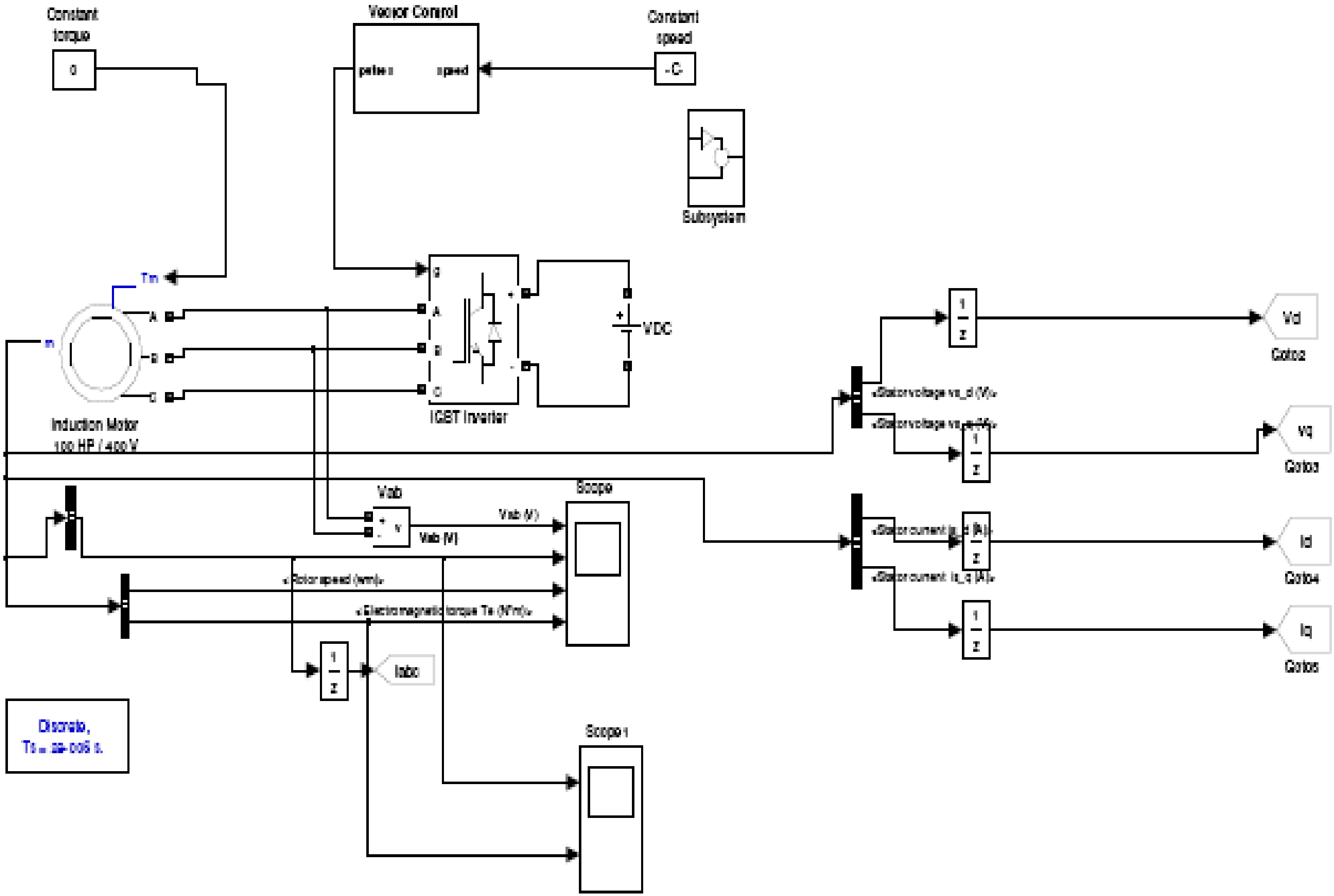
Constant torque
0
Vector Control
pulses
speed
Constant speed
-C-
Subsystem
Tm
A
B
C
Induction Motor
100 HP / 400 V
g
IGBT Inverter
VDC
Vab
Vab (V)
Scope
<Rotor speed (wm)>
1
z
Iabc
Scope1
Discrete,
Vd
Vq
Id
Iq

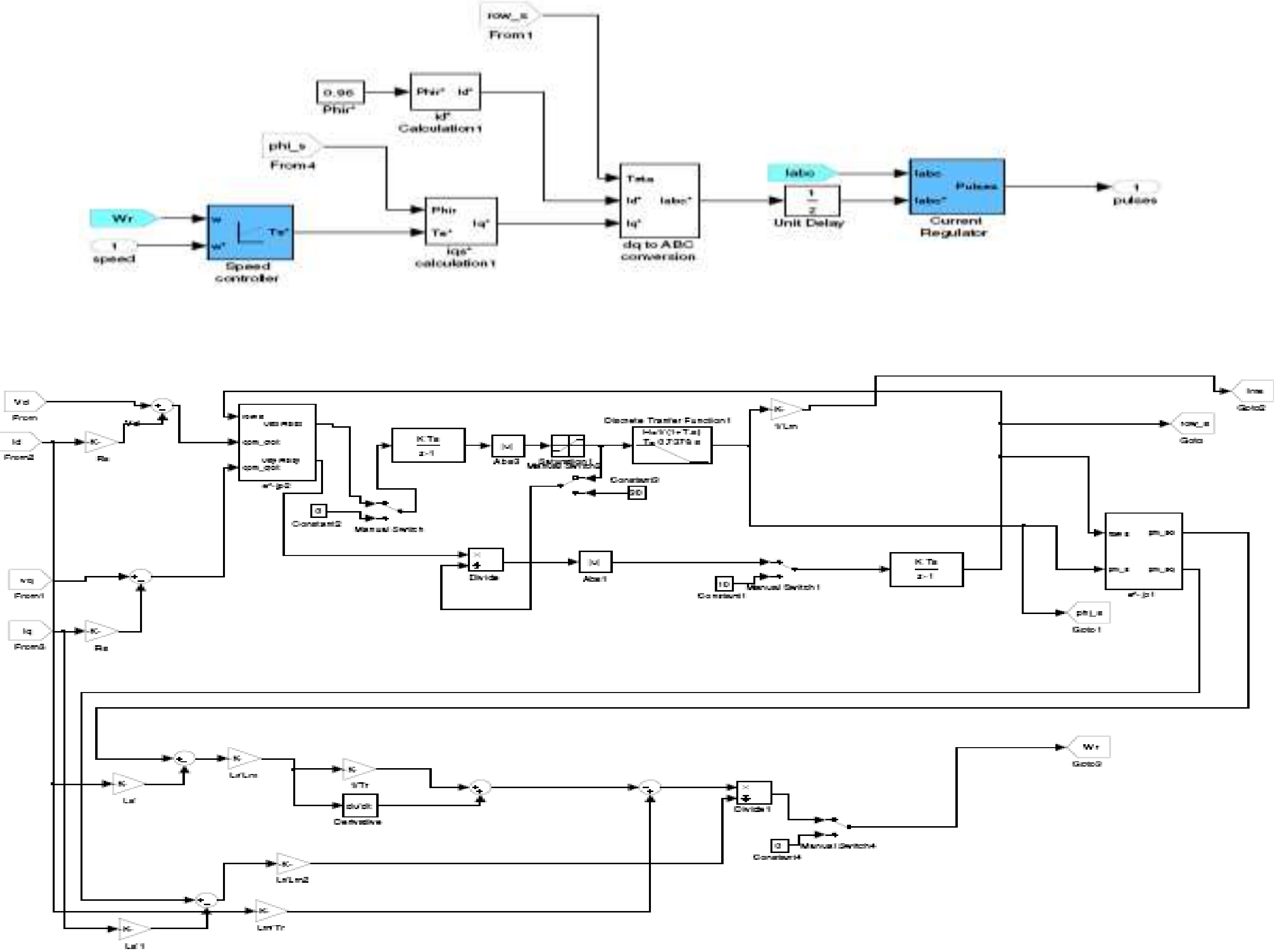

Figure 11. SFOC technique with simulink

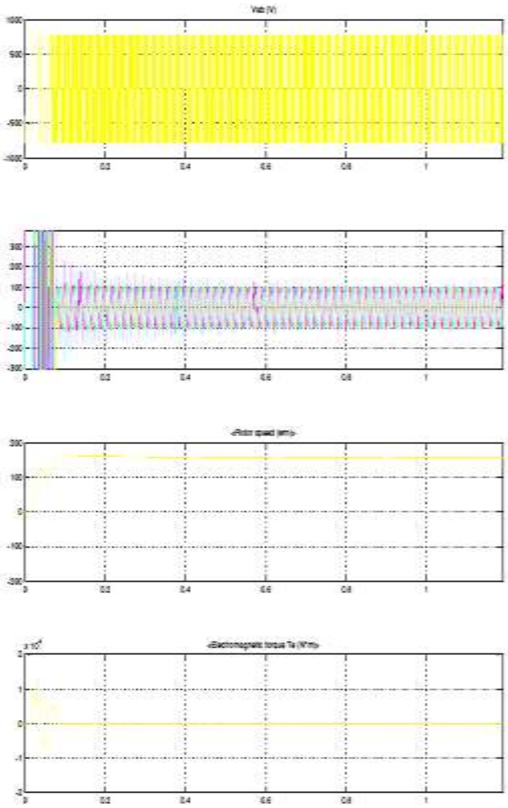

Figure 12 SFOC: V, I, N and T at 50 Hz

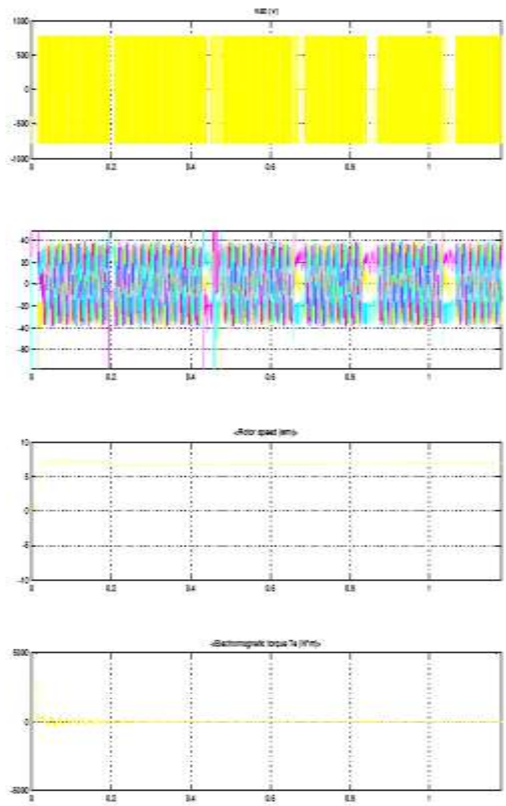

Figure 13 SFOC: V, I, N and T at 1 Hz

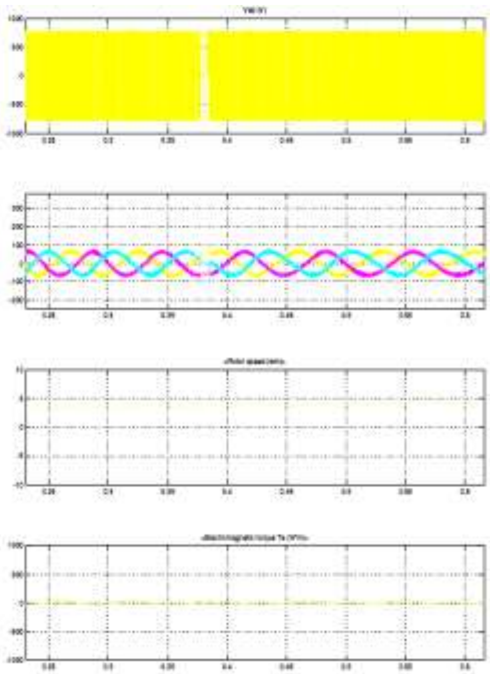

a.

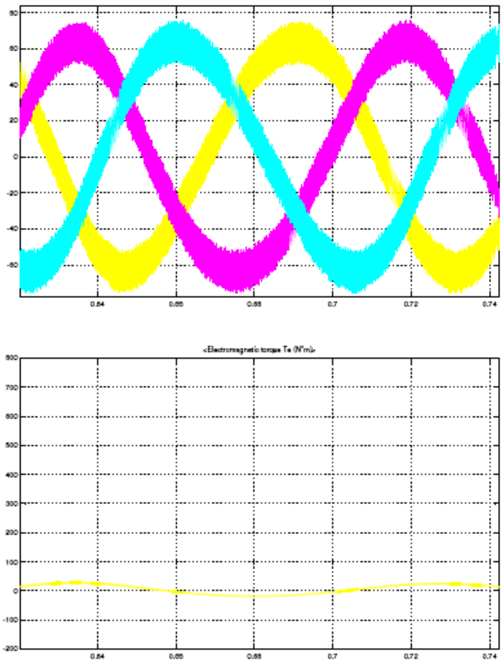

b.

Figure 14 a) SFOC: V, I, N and T at 1 Hz With the additional boost voltage b) SFOC: 1 and T at Hz With the additional boost voltage

Figure 14 shows the SFOC technique at 1 Hz. Due to stator resistance drop, the flux developed across the magnetic circuit is insufficient to develop the torque and increases the speed. For compensating flux reduction, a suitable amount of additional voltage is added to meet the flux requirement; it is developing more than required current with rated speed irrespective of load.

V. Experimental Results

Theoretical analysis and Experimentation results were carried out on 60t critical handling crane with hoist motion in up-ward direction. The motor details are shown in Table I. Table I shows the 100 HP induction motor parameters, based on the above parameters theoretical calculations are carried out.

Table 1. 60t VVVF drive based EOT crane motor details

Rated power	100 HP
Rated voltage	415V AC
Number of phase	3
Number of poles	8
Rated frequency	50 Hz
Line current	154 A
Rated speed	740 rpm
Rotor type	Squirrel cage
No load slip	0.9%
Stator resistance (R_1)	0.177 Ω
Stator reactance (X_1)	5.63 Ω
Magnetizing reactance (X_m)	10.89 Ω
Rotor resistance (R_2)	0.052 Ω
Rotor reactance (X_2)	7.92 Ω
VVVF Drive rating	75 kW

Figure 15 depicts the theoretical values between *v/f* and *slip/f* characteristics of 100 HP induction motor. From Figure15, it is observed that as frequency decreasing, voltage is decreasing and slip is increasing. This is due to Figure4 states that flux was constant below the rated frequency and shows that slip speed will be constant for constant torque. As the slip speed is constant below the rated frequency, slip was increasing with decrease in frequency. As the slip increases, rotor resistance referred to stator was decreasing with frequency thereby total impedance is decreasing so that voltage is decreasing in proportionate with stator impedance for constant motor torque. Figure 16 shows the theoretical and experimental results of 100 HP induction motor with encoder feedback. Theoretical and experimental values are matching with respect to voltage and current. From Figure16, it is observed that as frequency decreases, voltage was decreasing in linear up to 5 Hz, below 5 Hz, voltage variation was not linear due stator resistance voltage drop which is comparable with rotor resistance drop.

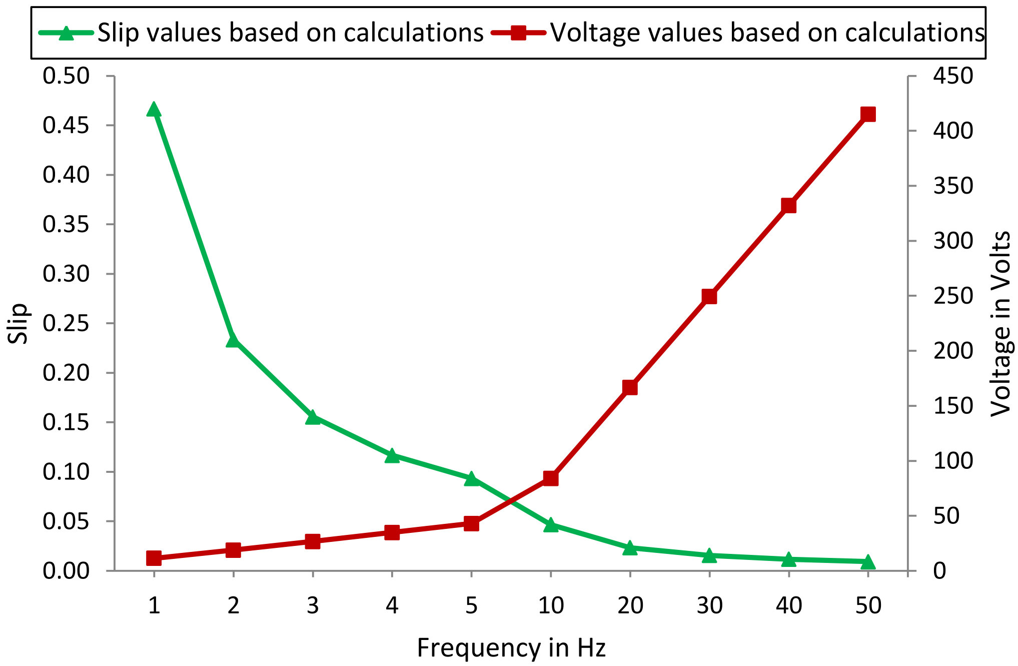

Figure 15. Theoretical results of 100 HP motor v/f and Slip/f characterstics

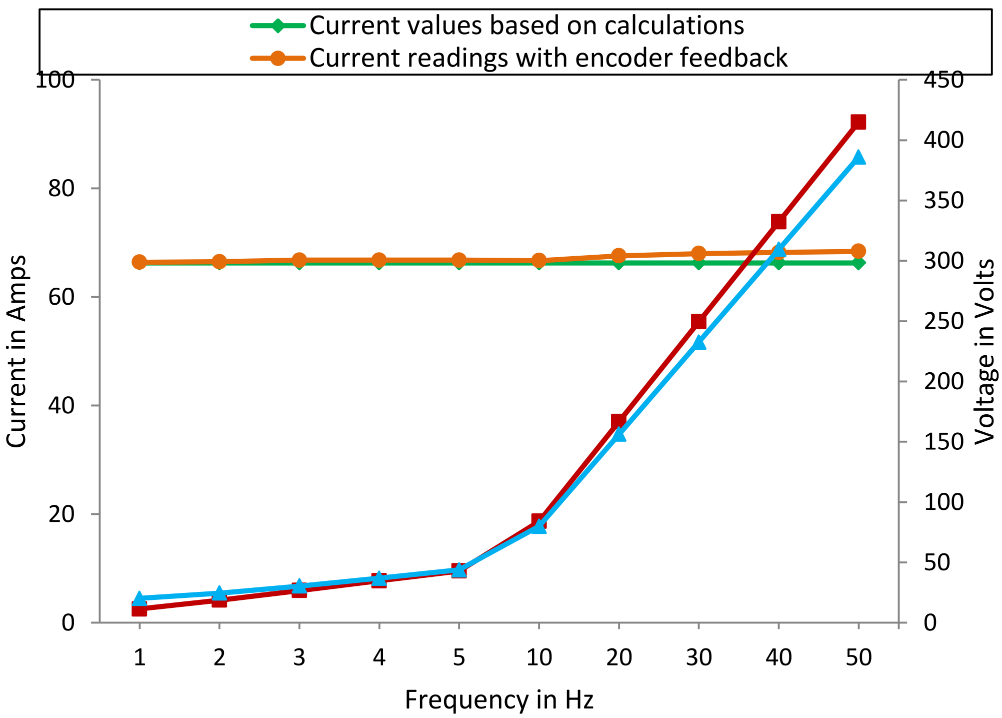

Figure16. Theoretical and experimental results of 100 HP motor v/f and i/f characteristics at no-load

Figure 17 shows the typical test results of *v/f* and *i/f* characteristics of 100 HP induction motor with and without encoder feedback. These modes resemble IFOC technique for with encoder and SFOC technique for without encoder. From Figure17, in SFOC technique, it is observed that at low frequency region i.e at 4 Hz, voltage is increased from 43.9 V to 50.7 V and current is raised from 66.8 A to 129.1 A. This incremental current is almost 43% to 84% of rated current from 5 Hz to 4 Hz. This increment is due to addition of boost voltage for compensating stator resistance drop. Continuous operation of motor with boost voltage will create more heat in stator and rotor conductors, causing torque pulsations and vibrations which will cause severe damage to motor. Whereas with encoder feedback, due to continuous monitoring of rotor angle and making slip speed as constant voltage is reduced from 43.9 V to 36.9 V from 5 Hz to 4 Hz and making current is 66.8A as constant. The reduction in voltage from 5 Hz to 4 Hz is not proportional due to adding of stator voltage drop compensation.

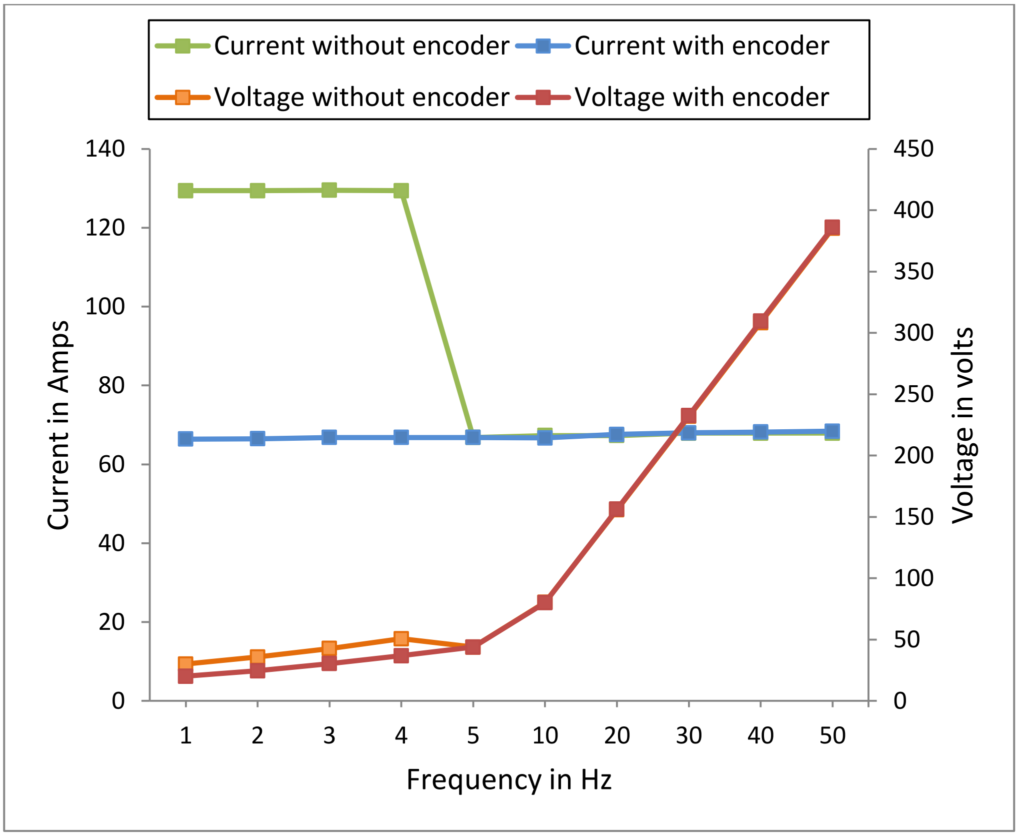

Figure 17. Typical Test results of 100 HP motor v/f and i/f characteristics with IFOC and SFOC techniques at no-load

Table 2 shows the comparison between IFOC and SFOC methods based on experimental results in low frequency region.

Table 2. Comparison of IFOC and SFOC methods in low frequency (0-5 Hz) region

Parameters	IFOC	SFOC
Dynamic response for torque	Quicker	Slower
Current	Only the motor current flows which is required for the actual torque.	Current impressed corresponds to the full load torque required, independent of the actual load torque at that time.
Voltage	Required voltage only will be applied to meet the actual torque.	Fixed voltage will be applied to meet the full load toque, independent of the actual load torque at that time.

Parameters	IFOC	SFOC
Feedback requirement	Encoder required.	No feedback
Speed Accuracy	More	Less
Magnetic saturation	Less	More
Thermal motor stressing	Lower	Higher
Vibration	Less	More
Bearing life	More	Less
Audible noise	Less	More
Complexity and process requirements	Higher	Lower

V. Conclusion

The aim of the paper was to give a fair comparison between IFOC and SFOC techniques at low frequency operation, to allow the users to identify the more suitable solution for any application that requires constant torque. The proposed techniques has been applied to 60t EOT crane having hoist motor capacity of 100 HP, three phase, squirrel cage induction motor. For 100 HP motor, *v/f* and *i/f* characteristics are demonstrated at low frequency region with IFOC and SFOC techniques. From simulation and experimental analysis, it is concluded that IFOC method is better technique than SFOC method in low frequency region.

VI. References

[1]. F. Blaschke, “A new method for the structural decoupling of A.C. induction machines,” in *Conf. Rec. IFAC,* Duesseldorf, Germany, Oct. 1971, pp. 1–15.

[2]. F. Blaschke, “The Principle of Field Orientation as Applied to the New Transvector Closed Loop Control for Rotating Machines”, *Siemens Rev.*, 1972, Vol.39, No. 5, pp. 217-220.

[3]. R.Gabriel, W.Leonhard and C.Nordby, “Field oriented control of standard AC motor using microprocessor”, IEEE Tran. IA, vol.16, no.2, pp.186-192, 1980.

[4]. Diana, G., Harley, R.G, "An Aid for Teaching Field Oriented Control Applied to Induction Machines", in IEEE Trans. Power Systems, Vol. 4, No. 3, pp. 1258-1262,1989.

[5]. Holtz, J, "The Representation of AC Machine Dynamics by Complex Signal Flow Graphs", in IEEE Trans. Ind. Appl., Vol. 42, No. 3, pp. 263-271, 1995.

[6]. Hasse, K. 1969. "Zur Dynamic Drehzahlgeregelter Antriebe Mit Stromrichter gespeisten Asynchron-Kuzschlublaufermaschinen", Ph. D. dissertation, Technische Hochschule Darmstadt, Darmstadt, Germany, 1969.

[7]. DeDoncker, R., Novotny, D.W., "The Universal Field Oriented Controller", in Conf. Rec. IEEE-IAS Annual Meeting, pp. 450-456, 1988.

[8]. DeDoncker, R., et al., "Comparison of Universal Field Oriented (UFO) Controllers in Different Reference Frames", in IEEE Trans. Power Electronics, Vol. 10, No. 2. pp. 205-213, 1995.

[9]. Vas, P, "Sensorless Vector and Direct Torque Control", Clarendon Press, Oxford, 1998.

[10]. Xu, X., Nowotny, D.W., "Implementation of Direct Stator Flux Oriented Control on a Versatile DSP Based System", in Conf. Rec. IEEE-IAS Annual Meeting, pp. 437-443, 1990.

[11]. Hopfensperger, D.J. Atkinson and R.A. Lakin, “Stator-flux-oriented control of a doubly-fed induction machine with and without position encoder” in *IEE 2000* pp: 241-250.

[12]. T. Ohtani, N. Takada, and K. Tanaka, “Vector control of induction motor without shaft encoder,” *IEEE Trans. Indust. Applicat.*, vol. 28, pp. 157–164, Jan./Feb. 1992.

[13]. I. Boldea and S. A. Nasar, *Vector Control of AC Drives*. Orlando, FL: CRC Press, 1992.

[14]. Bose, B.K., "Power Electronics and Drives", Prentice-Hall, Englewood Cliffs, New Jersey, 1986.

[15]. Radu Bojoi, Paolo Guglielmi and Gian-Mario Pellegrino, “Sensorless Direct Field-Oriented Control of Three-Phase Induction Motor Drives for Low-Cost Applications”, in *IEEE Trans. Indust. Applicat.*, vol.44, No.2, Mar./Apr. 2008.

[16]. X. Xu, R. DeDoncker, and D. W. Novotny, “A stator flux oriented induction machine drive,” in *Conf. Rec. PESC*, 1988, pp. 870–876.

[17]. Colin Schauder, “Adaptive Speed Identification for Vector Control of Induction Motors without Rotational Transducers”, in *IEEE Trans. Indust. Applicat.*, vol.28, No.5, Sept./Oct. 1992.

[18]. J. Maes and J. A. Melkebeek, “speed-sensorless direct torque control of induction motor using an adaptive flux observer,” *IEEE* Trans.*on Ind Appl*, vol. 36, no.3, pp. 778-785, 2000.

[19]. X. T. Garcia, B. Zigmund, A. Terlizzi , R. Pavlanin and L. Salvatore, “Comparison between FOC and DTC stratagies for permanent magnet synchronous motors”, in *Advances in Electrical and Electronic Engineering*, 2004, pp.76-81

[20]. Domenico Casadei, Francesco Profumo, Giovanni Serra and Angelo Tani, “FOC and DTC: Two Viable Schemes for Induction Motors Torque Control”, in IEEE *Trans. Power Electronics*, vol. 17, No.5, Sept. 2002, pp.779-787.

K. Seshubabu received the B.Tech degree in Electrical& Electronics engineering from JNTU, Hyderabad in 2002, and the M.E. degree in Electricalengineering with specialization in power electronics from R.G.P.V University, Bhopal, in 2005.He joined at Indian Space research Organisation (ISRO),Satish Dhawan Space Centre (SDSC), SHAR, Sriharikota in 2005. Since 2005, he has been with the SDSC, SHAR, as a Scientist/Engineer, where he is primarily responsible for realization of Electrical systems of GSLV Mk-III ground based facilities in SDSC.
His research interests include Variable Voltage Variable Frequency drives, SMPS topologies, power-factor correction and powersystems in general.
Currently he is supporting electrical systems for Mk-III integration activities and satellite propellant filling activities. He is a team member for Second Vehicle Assembly Building (SVAB) project.

C. L. Jose obtained his B.E Electrical Degree from Bangalore University and having 35 years of experience in various electrical power controls system area of ground based systems of Indian Space research Organisation (ISRO).He is instrumental in planning and realising various electrical systems at Satellite Centre, Bangalore, Satish Dhawan Space Centre, Sriharikota meeting requisite redundancy, reliability to meet successful space programs. His research interests include Variable Voltage Variable Frequency drives, Uninterrupted Power Supplies and power systems in general. Currently serving ISRO as Dy.General Manager for Electronics, Electrical and Checkout facilities for launch vehicles at SatishDhawan Space Centre, Sriharikota.